Asymptotic expansion of 1-dimensional sub-manifolds of stable and unstable manifolds in a 4-dimensional symplectic mapping

Yoshihiro Hirata[1] and Tetsuro Konishi
Department of Physics, Faculty of Science, Nagoya University,
Furo-cho, Chikusa-ku, Nagoya, 464-8602, Japan

Abstract

We analytically compute asymptotic expansions of a 1-dimensional sub-manifold of stable and unstable manifolds in a 4-dimensional symplectic mapping by using the method called *asymptotic expansions beyond all orders*. This method enables us to capture exponentially small splitting of separatrices and also to obtain explicit functional approximations of the sub-manifolds. In addition, we show the condition with which homoclinic structure caused by crossing between the stable and unstable sub-manifolds is regarded as a direct product of 2-dimensional mappings.

---

[1]e-mail address: yhirata@allegro.phys.nagoya-u.ac.jp

1 Introduction

Existence of transversal homoclinic (or heteroclinic) points implies non-integrability of Hamiltonian systems and it is important to understand homoclinic structure for studying phase space's structure of Hamiltonian systems. Melnikov's method (or Melnikov's integral) is a powerful tool to search for transversal homoclinic points[1]. This method is based on the regular perturbation method with respect to perturbation strength ϵ, hence it is difficult to apply this method to singular perturbed problems straightforwardly.

However in Hamiltonian systems with rapidly forces, and 2-dimensional symplectic mappings which are perturbations from the identical mappings, and so on, it is known that the homoclinic structure contains singular terms, for example, $\exp\left(-\beta/\epsilon^{\alpha}\right), \alpha, \beta > 0$ [2–4], and concequently had not been captured with the regular perturbation method with respect to ϵ.

The difficulty however have been overcome by using the method called *asymptotic expansions beyond all orders*. This method was first proposed and applied to the standard mapping by Lazutkin and co-workers[5]. They calculated intersecting angles between stable and unstable manifolds asymptotically. And the method was improved by using Borel transformation and Stokes phenomenon[6, 7]. The same approaches were developed independently by Kruskal and Segur[8] in the model of crystal growth and by Pomeau et al.[9] in the K-dV solitons under a 5-th order singular perturbation. Afterwards Tovbis et al. applied this method to Hénon map[10, 11] and constructed explicit functional approximations of the stable and unstable manifolds. Nakamura and Hamada analyzed a 2-dimensional symplectic mapping with a double well potential in the same way and calculated intersecting angles of stable and unstable manifolds[12].

The applications mentioned above are all to 2-dimensional symplectic mappings, which correspond to Poincaré mappings of Hamiltonian systems with two degrees of freedom. On the other hand, 4-dimensional symplectic mappings corresponds to Poincaré mappings of systems with three degrees of freedom. It is very impotant to extend the analytical method for 2-dimensional symplectic mappings to 4- or more-dimensional symplectic mappings, because phase space's structure of Hamiltonian systems with three or more degrees of freedom quite differs from that of systems with two degrees of freedom, e.g., Arnold diffusion[14].

An application to 4-dimensional symplectic mappings is reported by Gelfreich and Sharomov[13]. They treat a coupled 4-dimensional standard map and prove the splitting angle between 1-dimensional stable and unstable sub-manifolds is exponentially small and the splitting angle orthogonal to the sub-manifolds is not exponentially small. Their model however contains the particular coupling potential, i.e., two-body central force coupling $\tilde{J}(q_1 - q_2)$ (compare the mapping (1) or (6)).

We would like to take more general 4-dimensional mappings into consideration and construct functional approximations of 1-dimensional sub-manifolds of stable

and unstable manifolds. In this paper we shall show that it is possible to apply this method to more general coupling potential terms.

In this paper we consider a 4-dimensional symplectic map

$$
\begin{cases}
p_{j,n+1} &= p_{j,n} - \epsilon \left(2q_{j,n}^3 - q_{j,n} \right) - \epsilon^{\gamma+1} \kappa \dfrac{\partial \tilde{J}}{\partial q_{j,n}} \\
q_{j,n+1} &= q_{j,n} + \epsilon p_{j,n+1}
\end{cases}
\quad , \; j = 1, 2,
\tag{1}
$$

where $0 < \epsilon \ll 1$, $\kappa \in \mathbf{R}$, $\gamma \in \mathbf{N}$, and $\tilde{J} = q_{1,n}^{\alpha_1} q_{2,n}^{\alpha_2}$, $\alpha_1, \alpha_2 \in \mathbf{N}$ is a coupling term. The map (1) is an *exact symplectic map*, hence there exists a generating function $W = I + \epsilon J$ [15], where

$$
I = p_{j,n+1} q_{j,n},
\tag{2}
$$

$$
J = \sum_{j=1}^{2} \{ T(p_{j,n+1}) + V(q_{j,n}) \} + \epsilon^{\gamma} \kappa \tilde{J}(q_{j,n}),
\tag{3}
$$

$$
T(p) = \frac{1}{2} p^2,
\tag{4}
$$

$$
V(q) = \frac{1}{2} q^4 - \frac{1}{2} q^2.
\tag{5}
$$

And the map (1) is defined as $q_{j,n+1} = \partial W / \partial p_{j,n+1}$ and $p_{j,n} = \partial W / \partial q_{j,n}$. For $\epsilon = 0$ the map is obviously identical, hence the map (1) can be regarded as a perturbation from the 4-dimensional identical map. Note that the map (1) becomes chaotic when $\epsilon \neq 0$, in general.

The symplectic map (1) has a fully hyperbolic fixed point, which is a direct product of two of 2-dimensional hyperbolic fixed points, at the origin $(0, 0, 0, 0)$ (see the eqnation (5)). Hence there exist 2-dimensional stable and unstable manifolds near the origin.

In the present work we take $\alpha_1 = \alpha_2 = 2$, $\gamma = 2$, i.e., $\tilde{J} = q_{1,n}^2 q_{2,n}^2$ to simplify the following computation and notation. Thus the symplectic map (1) is rewritten as

$$
\begin{cases}
p_{j,n+1} &= p_{j,n} - \epsilon \left(2q_{j,n}^3 - q_{j,n} \right) - 2\epsilon^3 \kappa q_{j,n} q_{k,n}^2 \\
q_{j,n+1} &= q_{j,n} + \epsilon p_{j,n+1}
\end{cases}
\quad , \; j, k \in \{1, 2\}, \; j \neq k.
\tag{6}
$$

To construct the unstable manifold we transform the map (6) into the second order difference equations and change the independent variable n into t with meanings of time. We take ϵ as the difference parameter, that is, $q_{j,n\pm1} = q_j(t \pm \epsilon)$, $j = 1, 2$ if $q_{j,n} = q_j(t)$ [5, 10–12]. Thus

$$
\Delta_\epsilon^2 q_j(t) = q_j(t) - 2q_j(t)^3 - 2\epsilon^2 \kappa q_j(t) q_k(t)^2
\tag{7}
$$

where $\Delta_\epsilon^2 q_j(t) = \{ q_j(t + \epsilon) - 2q_j(t) + q_j(t - \epsilon) \} / \epsilon^2$, $j = 1, 2$.

One can transform the equations (7) into singular-perturbed ODEs[10–12],

$$\frac{d^2 q_j(t)}{dt^2} = q_j(t) - 2q_j(t)^3 - 2\epsilon^2\kappa q_j(t)q_k(t)^2 - 2\sum_{l=2}^{\infty} \frac{\epsilon^{2(l-1)}}{(2l)!}\frac{d^{2l}q_j(t)}{dt^{2l}} \tag{8}$$

One of the purposes of this paper is to construct explicit functional approximasions of 1-dimensional stable and unstable sub-manifolds which satisfy $q_1(t,\epsilon) = q_2(t,\epsilon)$.

An outline of constructing functional approximations of the sub-manifold, which is also an outline of this paper, is as follows: We construct solutions to the equations (8) with the regular perturbation method (section 2). The solutions however break down around $t \sim 0$ because of existence of singular points. Hence we blow up complex t-plane near one of the singular points and analyze with singular perturbation methods (section 3). One can rewrite the equations (7) near the singular points (section 4) as

$$\Delta^2\Phi_j = -2\Phi_j^3 + \epsilon^2\Phi_j - 2\kappa\epsilon^2\Phi_j\Phi_k^2, \tag{9}$$

where $\Delta^2\Phi_j(z) = \Phi_j(z+1) - 2\Phi_j(z) + \Phi_j(z-1)$, and $j, k \in \{1,2\}, j \neq k$. We analyze the equations (9) by using Borel transformation, which enables us to capture Stokes Phenomenon (section 5). We match the solutions of the equations (9) to the solutions of the equations (8) and successfully obtain the analytical representation of a 1-dimensional sub-manifold of an unstable manifold in the 4-dimensional symplectic mapping (section 6). Finally we will conclude the result (section 7) and give a summary of this paper in section 8.

2   The outer equation

In this section we try to construct a 1-dimensional sub-manifold of an unstable manifold of the equations (6) by using the regular perturbation method, i.e., Taylor expansion with respect to ϵ. Although the solution which satisfies the boundary conditions is obtained, it does not converge. We must therefore treat the equations (9) with the singular perturbation method in the next and following sections. Outline of construction of the manifold, which corresponds to contents from section 2 to section 6, goes along the way by Tovbis et al.[10, 11]. From now on, the subscripts j and k will be used as the meaning of $j, k \in \{1, 2\}, j \neq k$ without further comment.

First using Taylor expansions as

$$q_j(t \pm \epsilon) = \sum_{l=0}^{\infty} \frac{(\pm\epsilon)^l}{l!}\frac{d^l q_j(t)}{dt^l},$$

one can rewrite the equations (7) as

$$\frac{d^2 q_j(t)}{dt^2} = q_j(t) - 2q_j(t)^3 - 2\epsilon^2\kappa q_j(t)q_k(t)^2 - 2\sum_{l=2}^{\infty} \frac{\epsilon^{2(l-1)}}{(2l)!}\frac{d^{2l}q_j(t)}{dt^{2l}}. \tag{10}$$

3

Equations (10) and solutions to them are called *the outer equations* and *the outer solutions*, respectively. One can construct asymptotic representations of an unstable manifold as $t \to -\infty$ by solving the ODEs (10). Boundary conditions with which we solve the equations (10) are

$$\left.\begin{aligned}\lim_{t \to -\infty} q_{j,u}(t, \epsilon) &= 0 \\ q_{j,u}(t, \epsilon) &> 0\end{aligned}\right\}, \tag{11}$$

where the subscript u stands for an unstable manifold. The conditions (11) mean that the unstable manifold is asymptotic to the hyperbolic fixed point with positive value.

We construct a formal solution $\hat{q}_{j,0}(t, \epsilon)$ of the outer equations (10) in the power series of ϵ^2 as

$$\hat{q}_{j,0}(t, \epsilon) = \sum_{l=0}^{\infty} q_{j,0l}(t) \epsilon^{2l}, \tag{12}$$

which we call *the outer expansions*. Substituting the equations (12) into the equations (10), equations are successively obtained for each power of ϵ^2;

$$O(\epsilon^0) \quad : \quad \frac{d^2 q_{j,00}(t)}{dt^2} = q_{j,00}(t) - 2q_{j,00}(t)^3 , \tag{13}$$

$$O(\epsilon^{2l}) \quad : \quad \frac{d^2 q_{j,0l}(t)}{dt^2} = (1 - 6q_{j,00}(t)^2)q_{j,0l}(t) + F_{j,0l} \quad (l \geq 1), \tag{14}$$

where $F_{j,0l}$ are polynomials of $q_{m,00}(t), q_{m,01}(t), \cdots, q_{m,0,l-1}(t), m = 1, 2$ and their derivatives. The boundary conditions (11) are rewritten as

$$\left.\begin{aligned}\lim_{t \to -\infty} q_{j,0l}(t) &= 0 \\ q_{j,0l}(t) &> 0\end{aligned}\right\} \tag{15}$$

for $l = 0, 1, \cdots$.

From the equations (13) and (15) we obtain unperturbed solutions as

$$q_{j,00}(t) = \operatorname{sech}(t - t_j)$$

where t_js are integral constants.

In this paper we restrict our attention to a 1-dimensional sub-manifold which satisfies $q_{1,u}(t, \epsilon) = q_{2,u}(t, \epsilon)$, because it seems that construction of the whole 2-dimensional manifold is difficult. Hence one must put $t_1 = t_2$. Furthermore the system is autonomous; accordingly we can put $t_1 = t_2 = 0$ without loss of generality. Thus

$$q_{j,00}(t) = \operatorname{sech}(t). \tag{16}$$

4

The unperturbed solutions (16) possess even symmetry. Hence let us suppose that solutions of the outer equations (10) also possess the even symmetry, i.e.,

$$q_{j,u}(-t, \epsilon) = q_{j,u}(t, \epsilon), \ j = 1, 2. \tag{17}$$

Because the stable sub-manifold $q_{j,s}(t, \epsilon)$ is obtained as $q_{j,s}(t, \epsilon) = q_{j,u}(-t, \epsilon)$, if one can obtain consistent solutions of the equations (10) under the conditions (17), the stable and unstable sub-manifolds coincide perfectly, i.e., homoclinic bifurcation does not occur. Expanding the conditions (17) in the power of ϵ^2 one obtains

$$q_{j,0l}(-t) = q_{j,0l}(t), \ l = 0, 1, \cdots. \tag{18}$$

Next, by using the equations (16) we shall construct solutions for $O(\epsilon^2)$. The ODEs (14) are linear with inhomogeneous terms $F_{j,0k}$. Hence we construct homogeneous solutions first. They are linear combinations of two independent solutions $v_1(t)$ and $v_2(t)$ written as

$$v_1(t) = -\sinh(t)\operatorname{sech}^2(t), \tag{19}$$

$$v_2(t) = \frac{3}{2}\operatorname{sech}(t) - \frac{1}{2}\cosh(t) - \frac{3}{2}t\sinh(t)\operatorname{sech}^2(t). \tag{20}$$

Note that $v_1(t)$ and $v_2(t)$ are odd and even functions of t, respectively and Wronskian $W \equiv 1$. One can construct solutions to the equations (14) under the conditions (15) and (18) by using the equations (19) and (20);

$$q_{j,01}(t) = \frac{1}{3}\operatorname{sech}^3(t) - \frac{7 + 12\kappa}{24}\operatorname{sech}(t) + \frac{t}{24}\sinh(t)\operatorname{sech}^2(t). \tag{21}$$

In this way one can construct even solutions $q_{j,0l}(t)$, $l \geq 2$ successively.

This result leads to no homoclinic bifurcation, which is inconsistent with the fact that the symplectic map (6) becomes chaotic when $\epsilon \neq 0$. This indicates a breakdown of the application of the regular perturbation method (12). The breakdown can be clearly seen near the singular points of the outer solutions (16) and (21). We will discuss the breakdown in the next section.

3   The breakdown of the outer expansions

In this section we analyze the singular points of the outer solutions (16) and (21), extending the domain to complex t-plane.

The unperturbed solutions (16) have first order poles at $t = \pi i/2 + \pi i n$, $n \in \mathbf{Z}$. And the solutions for $O(\epsilon^2)$ (21) have third order poles at the same points. One can show that the solutions for $O(\epsilon^{2l})$ have the $(2l+1)$-th order poles (in general,

with ramification) at $t = \pi i/2 + \pi i n, \ n \in \mathbf{Z}$, i.e., for example, magnitude of $q_{j,0l}(t)$ in the neighborhood of $t = \pi i/2$ are given by

$$q_{j,0l}(t) \quad = \quad \frac{a_{j,l}}{(t - \pi i/2)^{2l+1}} \left(1 + O\left(\left| t - \frac{\pi}{2}i \right| \right) \right), \tag{22}$$

where $a_{j,l}$ are pure imaginary constants, for example, $a_{1,0} = a_{2,0} = -i$, $a_{1,1} = a_{2,1} = i/3$. By substituting the expressions (22) into the expansions (12) one obtain

$$
\begin{aligned}
\hat{q}_{j,0}(t, \epsilon) \quad &= \quad \sum_{l=0}^{\infty} q_{j,0l}(t)\epsilon^{2l} \\
&= \quad \sum_{l=0}^{\infty} \frac{a_{j,l}\epsilon^{2l}}{(t - \pi i/2)^{2l+1}} \left(1 + O\left(\left| t - \frac{\pi}{2}i \right| \right) \right).
\end{aligned} \tag{23}
$$

From the equations (23) one can see that all the terms in the expansions (12) give contributions of the same magnitude in $|t - \pi i/2| \sim \epsilon$ and that the regular perturbation method breaks down there. In the next section, we analyze the region near the singular points by blowing up there. The region are called *the inner region*, whereas the region in which the regular perturbation method is valid $(t \to -\infty)$ is called *the outer region*.

4   The inner equations

In the outer region we have obtained the even solution of the sub-manifold. This solution is valid in asymptotic of $t \to -\infty$, but near the singular points the asymptotic expansions (12) break down and one can't construct analytic continuation of $q_{j,u}(t, \epsilon)$ from the left half of t-plane to the right one. To construct the analytic continuation and capture odd parts of the manifold, we shall blow up near one of the singular points, $t = \pi i/2$ as

$$t - \frac{\pi}{2}i \quad = \quad \epsilon z. \tag{24}$$

In addition, we transform $q_j(t, \epsilon)$ to $\Phi_j(z, \epsilon)$ in order that the equations to solve possess no negative powers of ϵ as

$$\epsilon q_j(t, \epsilon) \quad = \quad \Phi_j(z, \epsilon). \tag{25}$$

By substituting the equations (24) and (25) into the equations (7), we obtain

$$\Delta^2 \Phi_j(z, \epsilon) \quad = \quad -2\Phi_j(z, \epsilon)^3 + \epsilon^2 \Phi_j(z, \epsilon) - 2\kappa\epsilon^2 \Phi_j(z, \epsilon)\Phi_k(z, \epsilon)^2, \tag{26}$$

where $\Delta^2 \Phi_j(z, \epsilon) = \Phi_j(z + 1, \epsilon) - 2\Phi_j(z, \epsilon) + \Phi_j(z - 1, \epsilon)$, The second order difference equations (26) are called *the inner equations*.

6

In this paper we try to construct the leading term of $\Phi_j(z, \epsilon)$, hence we restrict our attention only to the leading term of the inner equations, i.e.,

$$\Delta^2\Phi(z) = -2\Phi(z)^3. \tag{27}$$

We also call the equation (27) the inner equation[2].

5   The formal solution of the inner equation and Borel transformation

One can find the formal solution to the equation (27) around $z = \infty$ in the power series of $1/z$ as

$$\hat{\Phi}_0(z) = \sum_{l=0}^{\infty} \frac{a_l}{z^{2l+1}} \tag{28}$$

where $a_l \stackrel{\text{def}}{=} a_{1,l} = a_{2,l}$, $l = 0, 1, \cdots$ (see the equations (23)). Because $\hat{\Phi}_0(z)$ is a solution to the equation (27) with boundary condition $\hat{\Phi}_0(z) \to 0$ for $|z| \to \infty$, the coefficients a_l, $l = 0, 1, \cdots$ satisfy the following estimation[16]:

$$a_l \sim (-1)^{l+1} (2l+3)! \, (2\pi)^{-2l-2} \ (l \to \infty). \tag{29}$$

Although the radius of convergence of the right hand side of the equation (28) is obviously 0, $\hat{\Phi}_0(z)$ is an asymptotic expansion of $\Phi_u(z)$ for Re $z < 0$ and of $\Phi_s(z)$ for Re $z > 0$. Additionary $\hat{\Phi}_0(z)$ is Borel summable, i.e., the formal Borel transformation (the inverse Laplace transformation) of $\hat{\Phi}_0(z)$

$$\begin{aligned} V(p) &\stackrel{\text{def}}{=} L^{-1}\hat{\Phi}_0(z) \tag{30} \\ &= \sum_{l=0}^{\infty} \frac{a_l}{(2l)!}p^{2l} \end{aligned}$$

has a finite radius ($= 2\pi$) of convergence and the solution $\Phi(z) = LV(p)$ is known as the Borel sum of $\hat{\Phi}_0(z)$.

We hence apply the formal Borel transformation to the inner equation (27) and obtain

$$2(\cosh(p) - 1)V(p) = -2 \, [\, V * V * V \,](p), \tag{31}$$

where $V(p)$ has been defined as the equation (30) and convolution $[\, V * W * Y \,](p)$ is defined as

$$\begin{aligned} [\, V * W * Y \,](p) &\stackrel{\text{def}}{=} [\, [\, V * W \,] * Y \,](p) \\ &= [\, V * [\, W * Y \,] \,](p) \\ &= \int_0^p V(\tau) \int_0^{p-\tau} W(p - \tau - \lambda)Y(\lambda)d\lambda d\tau. \end{aligned}$$

---

[2]In [11] the leading equation of the inner equation is called *the truncated inner equation*. Here we call the equation (27) the inner equation for simplicity.

The solution to the integral equation (31) possesses poles only at $p = 2\pi ik$, $k \in$ $\mathbf{Z}\backslash\{0\}$[7]. Note that these singular points are determined by the kinetic terms of the generating function, hence in many physical problems this type of singular points appears.

One can define the unstable sub-manifold $\Phi_u(z)$ and the stable one $\Phi_s(z)$ by using the Laplace transformation as

$$\Phi_s(z) = \int_0^\infty e^{-pz}V(p)dp \ , \ |\arg z| < \pi, \tag{32}$$

$$\Phi_u(z) = \int_0^{-\infty} e^{-pz}V(p)dp \ , \ -2\pi < \arg z < 0, \tag{33}$$

respectively. Now let the difference between $\Phi_s(z)$ and $\Phi_u(z)$ be $\Phi_\pm(z)$ when $\pm\mathrm{Im}\ z > 0$, i.e.,

$$\Phi_\pm(z) \overset{\mathrm{def}}{=} \Phi_s(z) - \Phi_u(z) \ (\pm\mathrm{Im}\ z > 0). \tag{34}$$

From the equations (32) and (33) one obtains

$$i\ \mathrm{Im}\ \Phi_u(-i\zeta) = -\frac{1}{2}\Phi_-(-i\zeta), \tag{35}$$

where ζ is an arbitrary positive real number (see Appendix A).

Furthermore from the equations (32), (33) and (34) one obtains

$$\Phi_-(z) = \int_\gamma e^{-pz}V(p)dp \ (-\pi < \arg z < 0). \tag{36}$$

The integral path γ is shown in figure 1. $\Phi_-(z)$ is given as the sum of the residues of the poles on the positive imaginary semi-axis, i.e.,

$$\Phi_-(z) = 2\pi i \sum_{k=1}^\infty \mathrm{Res}[e^{-pz}V(p); p = 2\pi ik]. \tag{37}$$

Because of $|e^{-2\pi iz}| \gg |e^{-4\pi iz}| \gg \cdots$ in $\mathrm{Im}\ z < 0$, we shall only take account of the first term of the right hand side of the equation (37), i.e.,

$$\Phi_-(z) \sim 2\pi i\ \mathrm{Res}[e^{-pz}V(p); p = 2\pi i].$$

From the equation (37) one can realize that $\Phi_u(z)$ and $\Phi_s(z)$ possess the term in proportion to $e^{-2\pi ikz}$, hence we look for solutions to the equation (27) with the form

$$\overset{\circ}{\Phi}(z) = \sum_{l=0}^\infty \hat{\Phi}_l(z)e^{-2\pi ilz} \tag{38}$$

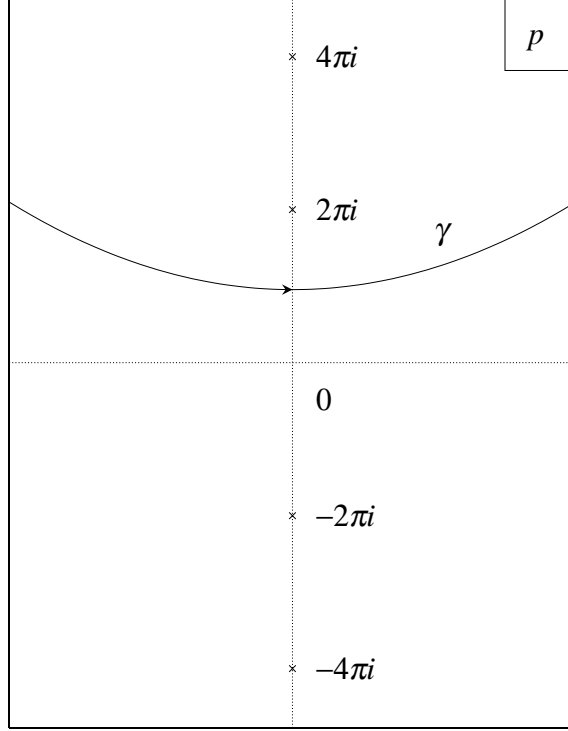$$= \hat{\Phi}_0(z) + \hat{\Phi}_1(z)e^{-2\pi iz} + \cdots.$$

Figure 1: The integral path γ on complex p plane is shown. One can take γ as enclosing the positive imaginary semi-axis.

By substituting the equation (38) into the equation (27), equations are successively obtained for each power of $e^{-2\pi i z}$;

$$O(e^0) \quad : \quad \Delta^2 \hat{\Phi}_0(z) = -2\hat{\Phi}_0(z)^3, \tag{39}$$

$$O(e^{-2\pi i z}) \quad : \quad \Delta^2 \hat{\Phi}_1(z) = -6\hat{\Phi}_0(z)^2 \hat{\Phi}_1(z), \tag{40}$$

$$\cdots.$$

The formal solution to the equation (39) has been obtained as the equation (28). In order to find the leading term of a solution to the equation (40), we replace $\hat{\Phi}_0(z)$ by its leading term $-i/z$. This yields

$$\Delta^2 \hat{\Phi}_1(z) = \frac{6}{z^2} \hat{\Phi}_1(z). \tag{41}$$

The equation (41) possesses two formal solutions $\hat{\Phi}_1^{even}(z)$, $\hat{\Phi}_1^{odd}(z)$ whose leading terms are z^{-2}, z^3, respectively. Because the odd solution $\hat{\Phi}_1^{odd}(z)$ dominates the even solution $\hat{\Phi}_1^{even}(z)$, we take account of only $\hat{\Phi}_1^{odd}(z)$, i.e., we replace $\hat{\Phi}_1(z)$ as $\hat{\Phi}_1^{odd}(z)$.

9

One can continue the process and obtain the formal solutions of $\hat{\Phi}_l$, $l \geq 2$. In this paper, however, we restrict our attention only to the first two terms of the equation (38), $\hat{\Phi}_0(z)$ and $\hat{\Phi}_1(z)$.

The odd solution $\hat{\Phi}_1^{odd}(z)$ possesses third order poles at $z = \infty$. Hence it is easily proved that $V(p)$ possesses fourth order poles at $p = 2\pi i k$, $k \in \mathbf{Z}$ by properties of Laplace transformation, i.e.,

$$
\begin{aligned}
V(p) &= L^{-1}\hat{\Phi}_0(z) \\
&\sim \frac{d_k}{(p - 2\pi i k)^4} + O\left(\frac{1}{|(p - 2\pi i k)^3|}\right), \quad d_k : \text{const}, \ k \in \mathbf{Z}.
\end{aligned} \tag{42}
$$

From the equation (42) we can obtain $\Phi_-(z)$ as

$$
\begin{aligned}
\Phi_-(z) &= 2\pi i \lim_{z \to 2\pi i} \frac{1}{3!} \frac{d^3}{dp^3}[(p - 2\pi i)^4 e^{-pz} V(p)] \\
&= c z^3 e^{-2\pi i z},
\end{aligned}
$$

where c ($= -2\pi i d_1/3!$) is a *Stokes constant* to be evaluated. There have been no analytical methods to evaluate the Stokes constant. However it is possible to estimate numerically by using the same algorithm as used in [9–12]. The result of our calculation shows $c \sim -796$.

By using the equation (35) one can let the coefficient of $bz^3 e^{-2\pi i z}$, which is the leading term of $\hat{\Phi}_{j,1}(z)$, as

$$
b = \begin{cases} 0 & , \quad -\pi < \arg z < -\dfrac{\pi}{2} \\ -\dfrac{c}{2} & , \quad \arg z = -\dfrac{\pi}{2} \\ -c & , \quad -\dfrac{\pi}{2} < \arg z < 0 \end{cases}, \tag{43}
$$

approximately.

6 Matching of the solutions

In this section we match the inner solutions to the outer solutions and construct the unstable sub-manifold which is valid on the right half of t-plane.

First we give the exponential expansions of the outer variables. Following the inner expansion (38), the refined outer expansions are given by

$$
\mathring{q}_j(t, \epsilon) = \hat{q}_{j,0}(t, \epsilon) + \hat{q}_{j,1}(t, \epsilon)e^{-\frac{2\pi i}{\epsilon}t} + \hat{q}_{j,2}(t, \epsilon)e^{-\frac{4\pi i}{\epsilon}t} + \cdots. \tag{44}
$$

Note that the exponential expansion (44) is singular with respect to ϵ, i.e., $e^{-\frac{2\pi i}{\epsilon}t}$ has essential singularity at $\epsilon = 0$.

The leading term of the expansion (44) has been obtained in section 2 as

$$\hat{q}_{j,0}(t,\epsilon) \;=\; q_{j,00}(t) + \epsilon^2 q_{j,01}(t) + O(\epsilon^4),$$

where

$$q_{j,00}(t) \;=\; \text{sech}(t), \tag{45}$$

$$q_{j,01}(t) \;=\; \frac{1}{3}\text{sech}^3(t) - \frac{7+12\kappa}{24}\text{sech}(t) + \frac{1}{24}t\sinh(t)\text{sech}^2(t). \tag{46}$$

Next we construct the first exponential terms $\hat{q}_{j,1}(t,\epsilon)$, which correspond to $O(e^{-\frac{2\pi i}{\epsilon}t})$. Substituting the expansions (44) into the equations (7) gives

$$\Delta_\epsilon^2 \hat{q}_{j,1}(t,\epsilon) \;=\; (1 - 6\hat{q}_{j,0}(t,\epsilon)^2)\hat{q}_{j,1}(t,\epsilon) - 2\epsilon^2\kappa\hat{q}_{j,0}(t,\epsilon)\hat{q}_{k,0}(t,\epsilon)^2.$$

To estimate the leading order of $q_{j,10}(t)$, which is the leading term of $\hat{q}_{j,1}(t,\epsilon)$, we replace $\hat{q}_{j,0}(t,\epsilon)$ with their leading term $q_{j,00}(t)$. By these replacements, we obtain the differential equations of $q_{j,10}(t)$ as

$$\frac{d^2 q_{j,10}(t)}{dt^2} \;=\; (1 - 6q_{j,00}(t)^2)q_{j,10}(t). \tag{47}$$

The general solutions of the equations (47) are given as

$$q_{j,10}(t) \;=\; c_{j,1}v_1(t) + c_{j,2}v_2(t),$$

where $c_{j,1}$ and $c_{j,2}$ are arbitrary constants, and $v_1(t)$ and $v_2(t)$ are given by the equations (19) and (20).

We rewrite functions $v_1(t)$ and $v_2(t)$ in the neighborhood of the singular point $t = \pi i/2$. If we introduce $\delta = t - \pi i/2$, the equations (19) and (20) imply

$$v_1(t) \;=\; i\frac{\cosh(\delta)}{\sinh^2(\delta)}, \tag{48}$$

$$v_2(t) \;=\; \frac{3}{4}\pi i v_1(t)$$
$$-\frac{1}{2}i\frac{1}{\sinh^2(\delta)}[\,3\sinh(\delta) + \sinh^3(\delta) - 3\delta\cosh(\delta)\,]. \tag{49}$$

One can see that the odd function $v_1(t)$ becomes an even function of δ and the even function $v_2(t)$ has both odd and even parts. The leading term of $v_1(t)$ around $\delta = 0$ is of the order $O(\delta^{-2}) = O(\epsilon^{-2}z^{-2})$. It corresponds to the solution $\hat{\Phi}_1^{even}(z)$ of equation (41), which is sub-dominant to the other solution $\hat{\Phi}_1^{odd}(z)$. The odd part of $v_2(t)$, which is in the square bracket, has the Taylor expansion as

$$3\sinh(\delta) + \sinh^3(\delta) - 3\delta\cosh(\delta)$$
$$=\; 0\cdot\delta + 0\cdot\delta^3 + \frac{2}{5}\delta^5 + O(\delta^7).$$

11

The coefficient of the square bracket is of the order $O(\delta^{-2})$. These show that the odd part of the equation (49) is of the order $O(\delta^3)$ $(= O(\epsilon^3 z^3))$, corresponding to $\hat{\Phi}_1^{odd}(z)$. We shall therefore match $q_{j,10}(t)$ to $\hat{\Phi}_1(z) \equiv \hat{\Phi}_1^{odd}(z)$, i.e., $q_{j,10}(t)$ is given by the odd part of $v_2(t)$ as

$$q_{j,10}(t) = c_{j,2}\left[v_2(t) - \frac{3}{4}\pi i v_1(t)\right] \tag{50}$$

$$= -\frac{1}{5}c_{j,2}i\delta^3(1 + O(\delta^2))$$

$$= -\frac{1}{5}c_{j,2}i\epsilon^3 z^3(1 + O(\delta^2)).$$

Furthermore the discussion in section 5 shows

$$i \, \text{Im} \, \Phi_u(z) \sim bz^3 e^{-2\pi iz}$$

where b has been determined as the equation (43). The matching $q_{j,10}(t)$ and $\hat{\Phi}_1^{odd}(z)$ for t approaching $\pi i/2$ with $\arg z = -\pi/2$ is given below:

$$\epsilon q_{j,10}(t)\exp\left(-\frac{2\pi it}{\epsilon}\right) = -\frac{1}{2}cz^3 e^{-2\pi iz},$$

hence,

$$c_{j,2} = -\frac{5}{2}i\frac{c}{\epsilon^4}\exp\left(-\frac{\pi^2}{\epsilon}\right), \tag{51}$$

where $c \in \mathbf{R}$, therefore, $c_{j,2} \in i\mathbf{R}$. Another constant $c_{j,1}$ is given as

$$c_{j,1} = \frac{3}{4}\pi i c_{j,2}$$

$$= \frac{15}{8}\pi\frac{c}{\epsilon^4}\exp\left(-\frac{\pi^2}{\epsilon}\right)$$

(see equation (50) and (51)).

Finally, the leading term of the imaginary part of the sub-manifold $q_{j,10}(t)$ is given as

$$q_{j,10}(t) = c_{j,1}v_1(t) + c_{j,2}v_2(t)$$

$$= -\frac{1}{2}ic_{j,2}\frac{1}{\sinh^2(\delta)}[3\sinh(\delta) + \sinh^3(\delta) - 3\delta\cosh(\delta)]$$

$$= \frac{c_{j,2}}{2}\left[3(t - \frac{\pi}{2}i)\sinh(t)\text{sech}^2(t) - 3\text{sech}(t) + \cosh(t)\right].$$

7 Results

We have constructed the solutions which are valid in the neighborhood of the singular point $t = \pi i/2$. The same arguments, applied to the complex conjugated singular point $t = -\pi i/2$, yield the complex conjugated solutions. We take the two singular points, which are nearest to the real axis, into consideration and restore the obtained solutions to real functions. Taking the average of these two solutions, we obtain

$$\overset{\circ}{q}_j (t, \epsilon) = \hat{q}_{j,0}(t, \epsilon) + \mathrm{Re}\left[\sum_{l=1}^{\infty} \hat{q}_{j,l}(t, \epsilon)\exp\left(-\frac{2\pi i l}{\epsilon}t\right)\right].$$

In this paper we approximate the sub-manifold by taking the term $l = 1$. This term is written as

$$\begin{aligned}
\mathrm{Re}\left[\hat{q}_{j,1}(t, \epsilon)\exp\left(-\frac{2\pi i t}{\epsilon}\right)\right] &\sim \mathrm{Re}\left[q_{j,10}(t)\exp\left(-\frac{2\pi i t}{\epsilon}\right)\right] \\
&= c_1 v_1(t)\cos\frac{2\pi t}{\epsilon} - i c_2 v_2(t)\sin\frac{2\pi t}{e} \\
&= M(t, \epsilon)B(t, \epsilon)
\end{aligned}$$

where

$$M(t, \epsilon) = -S(t, \epsilon)\frac{5}{2}\frac{c}{\epsilon^4}\exp\left(-\frac{\pi^2}{\epsilon}\right), \tag{52}$$

$$B(t, \epsilon) = \frac{3}{4}\pi v_1(t)\cos\frac{2\pi t}{\epsilon} - v_2(t)\sin\frac{2\pi t}{\epsilon}. \tag{53}$$

The switching function $S(t, \epsilon)$, which stands for Stokes phenomenon, is approximately given as

$$S(t, \epsilon) = \begin{cases} 0 & (t < 0) \\ 1 & (t = 0) \\ 2 & (t > 0) \end{cases} \tag{54}$$
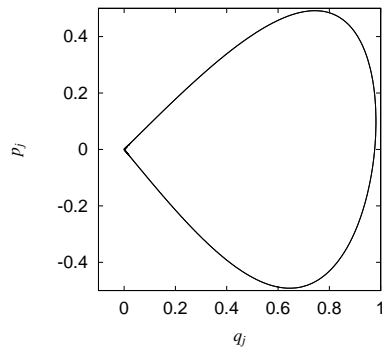
(see the equations (43) and (52)).

By using these functions, the parametrization of the unstable sub-manifold is

$$\tilde{q}_{j,u}(t, \epsilon) = q_{j,00}(t) + \epsilon^2 q_{j,01}(t) + M(t, \epsilon)B(t, \epsilon), \tag{55}$$
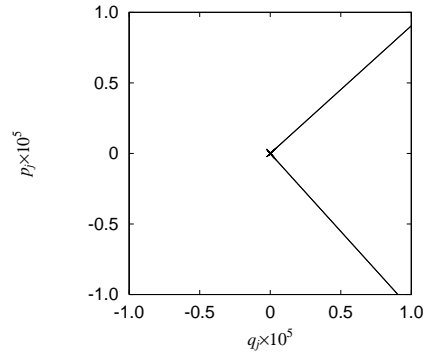
and the momentum variables $\tilde{p}_{j,u}(t, \epsilon)$ is given as

$$\tilde{p}_{j,u}(t, \epsilon) = \frac{\tilde{q}_{j,u}(t, \epsilon) - \tilde{q}_{j,u}(t - \epsilon, \epsilon)}{\epsilon} \tag{56}$$
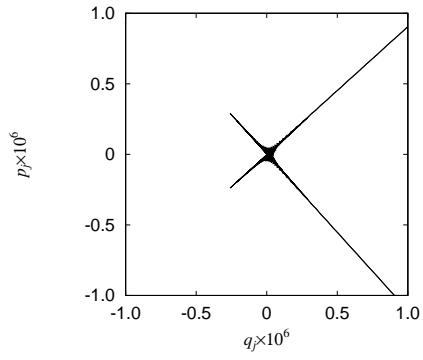
(see the equation (6)). On the other hand, the parametrization of the stable sub-manifold is given as $\tilde{q}_{j,s}(t, \epsilon) = \tilde{q}_{j,u}(-t, \epsilon)$ and $\tilde{p}_{j,s}(t, \epsilon) = -\tilde{p}_{j,u}(-t + \epsilon, \epsilon)$.
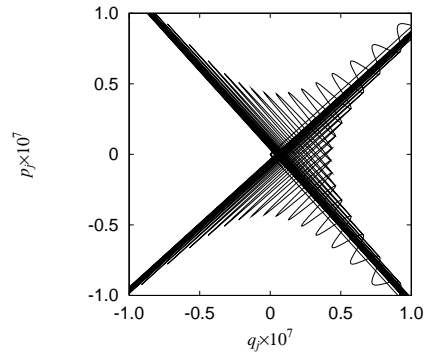
13

Figure 2: The functional approximations of the stable and unstable sub-manifolds projected on (q_j, p_j) plane. The parameters are $\epsilon = 0.2$, $\kappa = 1.0$.

By using the equations (56) one can observe the manifold on the phase space. However it is impossible to display a 4-dimensional phase space graphically, hence we observe its projections to (q_1, p_1) and (q_2, p_2) plane. From equations (55), (45) and (46) the projections to (q_1, p_1) and (q_2, p_2) plane are same. Figure 2,(a) shows that global shapes of the stable and unstable sub-manifolds. In figure 2,(b)–(d) we magnify the neighborhood of the fixed point. One can clearly see the homoclinic structure from figure 2,(d).

Next we compare the approximate solution (55) and (56) with numerical trajectories. 20 numerical trajectories are plotted on figure 3. This figure shows
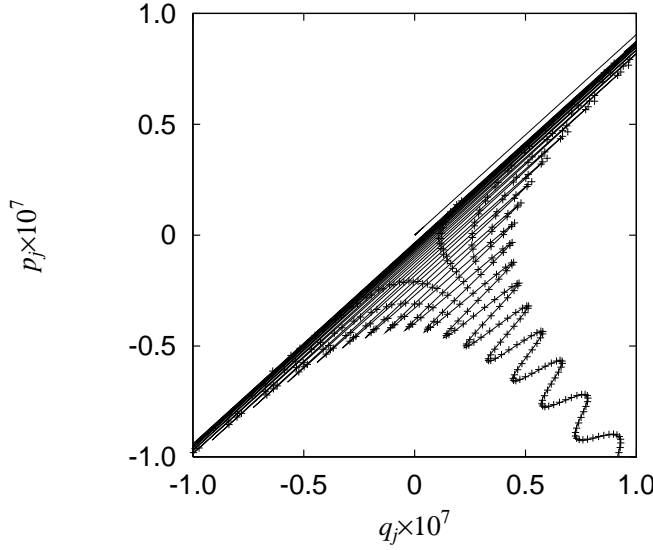

Figure 3: The comparison between the approximate solution of the unstable sub-manifold and 20 numerical trajectories. The parameters are same as figure 2. The initial values of the numerical trajectories are given on the solution between $t = 14.0$ and $t = 14.2$ with equal intervals.

that the approximate solution agree well with the numerical trajectories. The initial values of the numerical trajectories are given on the approximate solutions between $t = 14.0$ and $t = 14.2$ with equal intervals, i.e., $t = 14.0$, $t = 14.005$, $\cdots$, $t = 14.195$. In other values of ϵ or κ also one can show that the approximate solution agree well with numerical solutions.

8 Summary and discussions

We extended the method *"asymptotic expansions beyond all orders"* for the 4-dimensional symplectic mapping (6) straightforwardly and successfully obtained

the explicit functional approximation of the 1-dimensional sub-manifolds of the stable and unstable manifolds (55). These asymptotic solutions well approximate numerical solutions in the neighborhood of the hyperbolic fixed point, which is important to understand phase space's structure of Hamiltonian systems. We therefore consider that by this extension one can analyze global structure of phase space of Hamiltonian systems with three degree of freedom.

The oscillating parts $M(t, \epsilon)$ and $B(t, \epsilon)$ do not contain the coupling constant κ (see the equations (52) and (53)). This indicates that the homoclinic structure is a direct product of 2-dimensional symplectic mappings. In other words, the model we analyzed shows only quantitative characteristic properties of high-dimensionality. This is based on the fact that the inner equation (27) is decoupled. From the order of the singular points of the outer solutions, we find the condition that the coupling term dominates the nonlinear terms. The condition is written as

$$\begin{cases} \alpha_1 + \alpha_2 & < & \gamma + 4 & \cdots & \text{decouple} \\ \alpha_1 + \alpha_2 & > & \gamma + 4 & \cdots & \text{coupling term dominates} \end{cases} \tag{57}$$

(see the map (1) and appendix B). When the second condition of the conditions (57) is satisfied, the coupling term dominantly contributes the inner equations and another type of rescaling (see equations (24) and (25)) is required. Hence we consider that the models whose coupling terms satisfy the second condition make not only quantitative but also qualitative differences. However it is impossible to treat such models with the same way. We would like to improve this method in order to extend to such models in a future work.

In the present work we have restricted our attention to the particular 1-dimensional sub-manifolds of the stable and unstable manifolds. And we have shown that the sub-manifolds oscillate in the vicinity of the origin. Because the unstable sub-manifold is contained in the unstable manifold, it is clear that the unstable manifold itself oscillates. We now try to construct explicit functional approximations of the whole 2-dimensional stable and unstable manifold[17].

In the present model there exists a 4-dimensional fully hyperbolic fixed point (a direct product of two 2-dimensional hyperbolic fixed points). In a future work we will extend this method to 4-dimensional symplectic mappings with a hyperbolic×elliptic type fixed point.

Acknowledgements

References

[1] Guckenheimer J and Holmes P 1983 *Nonlinear oscillations, dynamical systems, and bifurcations of vector fields* (New York: Springer)

[2] Neishtadt A I, 1984 *J. Appl. Math. Mech.* **48**(2) 133

[3] Lazutkin V F, Schachmannski I G and Tabanov M B 1989 *Physica* **40D** 235

[4] Amick C, Ching E S, Kadanoff L P and Rom-kedar V 1992 *J. Nonlinear Sci.* **2** 9

[5] Gelfreich V G, Lazutkin V F and Svanidze N V 1994 *Physica* **71D** 82

[6] Hakim V and Mallick K 1993 *Nonlinearity* **6** 57

[7] Tovbis A 1994 *Commun. Math. Phys.* **163** 245

[8] Kruskal M D and Segur H 1991 *Stud. Appl. Math.* **85** 129

[9] Pomeau Y, Ramani A and Grammaticos B 1988 *Physica* **31D** 127

[10] Tovbis A, Tsuchiya M and Jaffé C 1994 *preprint*

[11] Tovbis A, Tsuchiya M and Jaffé C 1998 *Chaos* **8** 665

[12] Nakamura K and Hamada M 1996 *J. Phys., A* **29** 7315

[13] Gelfreich V G and Sharomov D K 1995 *Phys. Lett. A* **197** 139

[14] Arnold V I 1964 *Soviet Math. Dokl.* **5** 581

[15] Delshams A and Ramírez-Ros R 1997 *Commun. Math. Phys.* **190** 213

[16] Suris Y B 1994 *Nonlinearity* **7** 1225

[17] Hirata Y and Nozaki K *In preparation*

A The imaginary part of $\Phi_u(z)$

In this appendix we prove equation (35). From equations (32) and (33) we obtain

$$
\begin{aligned}
\Phi_u(-z) &= \int_0^{-\infty} e^{pz} V(p) dp \\
&= \int_0^{\infty} e^{-pz} V(-p)(-dp) \\
&= -\Phi_s(z),
\end{aligned}
$$

and

$$
\Phi_s(\bar{z}) = -\bar{\Phi}_s(z).
$$

Assume $\zeta \in \mathbf{R}$. One can easily prove that

$$
\Phi_u(-i\zeta) = -\Phi_s(i\zeta) = \bar{\Phi}_s(-i\zeta).
$$

Furthermore assume $\zeta > 0$, and Φ_s and Φ_u are real-valued on the negative imaginary semi axis, one can obtain

$$\Phi_u(-i\zeta) \;=\; \bar{\Phi}_s(-i\zeta) \;=\; \Phi_s(-i\zeta), \tag{58}$$

$$\Phi_u(i\zeta) \;=\; -\Phi_s(-i\zeta) \;=\; -\bar{\Phi}_s(-i\zeta) \;=\; \Phi_s(i\zeta). \tag{59}$$

By using equation (58) and equation (59), we can say that

$$\Phi_s(z) \;\equiv\; \Phi_u(z) \; (z \in i\mathbf{R}).$$

Hence Re $\Phi_s(z) = $ Re $\Phi_u(z)$ on the imaginary axis: i.e.,

$$\Phi_\pm(z) \;\in\; i\mathbf{R} \; (z \in i\mathbf{R}).$$

Particularly when $\zeta > 0$, from equation (58) one can obtain

$$\begin{aligned}
\Phi_-(-i\zeta) \;&=\; \Phi_s(-i\zeta) - \Phi_u(-i\zeta) \\
&=\; -2i \; \text{Im} \; \Phi_u(-i\zeta).
\end{aligned}$$

Thus

$$i \; \text{Im} \; \Phi_u(-i\zeta) \;=\; -\frac{1}{2}\Phi_-(-i\zeta).$$

B   The order of the coupling term

In this appendix we study the order of the coupling terms in the map (1). The coupling term is generated by $\epsilon^\gamma \tilde{J} = \epsilon^\gamma q_{1,n}^{\alpha_1} q_{2,n}^{\alpha_2}$, $\alpha_j \in \mathbf{N}$, $j = 1, 2$.

Put $A = \alpha_1 + \alpha_2$. First let us suppose $\gamma = 2$. The outer solutions of $O(\epsilon^2)$ are written as

$$\begin{aligned}
q_{j,01}(t) \;=\; & \frac{1}{3}\text{sech}^3(t) - \frac{7}{24}\text{sech}(t) \\
& +\frac{t}{24} \; \sinh(t)\text{sech}^2(t) + \kappa\alpha_j C(t; A),
\end{aligned} \tag{60}$$

$$C(t; A) \;=\; \begin{cases}
\dfrac{1}{3}\text{sech}^2(t) & (A = 3) \\[2ex]
\dfrac{1}{A}\dfrac{(A-4)!!}{(A-5)!!} & \\
\quad \times \displaystyle\sum_{k=1}^{M} \dfrac{(A-5-2k)!!}{(A-2-2k)!!}F(t; -A+1+2k) & (A \geq 4)
\end{cases} \tag{61}$$

18

where $(2n)!! = 2n \cdot (2n-2) \cdots 2$, $(2n-1)!! = (2n-1) \cdot (2n-3) \cdots 1, n \in \mathbf{N}$, $0!! = (-1)!! = 1$, $(-2)!! = (-3)!! = -1$, and $F(t;n), n \in Z$ is defined as

$$F(t;n) = \begin{cases} \cosh^n(t) & (n \geq 1) \\ \sinh(t)\operatorname{sech}^2(t)\operatorname{gd}(t) & (n = 0) \end{cases}, \tag{62}$$

$$\operatorname{gd}(t) = \tan^{-1}(\sinh(t))$$

and

$$M \stackrel{\text{def}}{=} \left[\frac{A}{2}\right] - 1 \tag{63}$$

$$= \begin{cases} \dfrac{A}{2} - 1 & \cdots \quad A : \text{even} \\ \dfrac{A+1}{2} - 2 & \cdots \quad A : \text{odd} \end{cases}.$$

From equations (60)–(63) one sees that when $A \geq 6$ the outer solutions $q_{j,01}(t)$, $j = 1, 2$ possess singularities of the order $A-3 (\geq 3)$ at $t = \pi i/2 + \pi i k$, $k \in \mathbf{Z}$ (in general, with ramification). On the other hand, when $A < 6$, the order of the singularities is 3. One can easily prove that the outer solutions of $O(\epsilon^{2k})$ possess singularities of the order $k(A-4) + 1$ or $2k+1$ when $A \geq 6$ or $A < 6$, respectively. Hence if $A \geq 6$, the magnitude of $q_{j,0k}(t)$ in the neighborhood of $t = \pi i/2$ are given by

$$q_{j,0k}(t) = \frac{a_{j,k}}{(t - \pi i/2)^{k(A-4)+1}}\left(1 + O\left(\left|t - \frac{\pi}{2}i\right|\right)\right), \tag{64}$$

$$a_{j,k} \in \mathbf{C}, \ j = 1, 2, \ k \geq 0.$$

From equations (64) one can realize that all the terms in the formal expansions (12) give contributions of the same order in $|t - \pi i/2| \sim \epsilon^\delta, \delta = \frac{2}{A-4}$. We must therefore blow up near the one of the singular points, $t = \pi i/2$ as

$$t - \frac{\pi}{2}i = \epsilon^\delta z$$

(compare equation (24) and the discussions in section 3). Note that if $A > 6$, then $\delta < 1$, hence $\epsilon^\delta > \epsilon$, that is, the inner region is wider with $A > 6$ than with $A \leq 6$.

Now we show that when $\gamma = 2$ and $A > 6$, the rescaling factor is different from that of $A \leq 6$. Hence we call the models with $A > 6$ or $A \leq 6$ *strongly* or *weakly coupled model*, respectively. In the same way, one can prove that the condition with which the rescaling factor is different from 2-dimensional mappings (storongly coupled model) is written as

$$\alpha_1 + \alpha_2 > \gamma + 4 \tag{65}$$

for general $\gamma \in \mathbf{N}$.